

Synthesis and Characterisation of Transition Metal Complexes Derived from 4-Aminoantipyrine and Thiosemicarbazide Based Schiff Base

N.M.Abdul khaderJailani^a, A.Xavier^{b,*} and A.Ramu^c

^aDepartment of Chemistry, HKRH College, Uthamapalayam-625533, Tamil Nadu, India

^{b,*}Department of Chemistry, The Madura College, Madurai -625011, Tamil Nadu, India

^cDepartment of Inorganic Chemistry, Madurai Kamaraj University, Madurai -625021, Tamil Nadu, India

Abstract

A novel Schiff base ligand was synthesized through the condensation of 4-Aminoantipyrine with 1, 3-isophthalaldehyde and Thiosemicarbazide. The Schiff base ligand and its metal complexes of Co(II), Ni(II), Cu(II) and Zn(II) were synthesized and characterized by elemental analyses, molar conductance, magnetic susceptibility measurement, IR, UV-Vis, ¹H NMR, Mass and EPR spectral studies. The data showed that the complexes have composition of [ML]Cl₂ stoichiometry. The conductivity data confirmed the electrolytic nature of the complexes. The metal complexes of Co (II), Ni (II), and Zn (II) were showed an octahedral configuration. The electronic absorption spectra of the Cu (II) complex suggested a square-planar geometry around the central metal ion further it was confirmed by the EPR spectrum. The IR spectral data suggest the involvement of sulphur and azomethine nitrogen in coordination to the central metal ion. The interaction of the complexes with calf thymus (CT) DNA has been studied using absorption spectra and Cyclic Voltammetric measurement. The metal complexes exhibit effective cleavage of pBR 322 DNA from the super coiled form to the open circular form. The synthesized complexes have been subjected to antimicrobial study. The antimicrobial results indicated that the antimicrobial activity of the complexes show the enhanced activity in comparison to free ligand. These findings are giving suitable support for developing new anti cancer and antimicrobial agent and expand our scope for applications.

* Corresponding author:
jailani150677@gmail.com

Received 25 Dec 2017,

Revised 01 Nov 2018,

Accepted 20 Dec 2018

Keywords: 4-aminoantipyrine; Schiff base ligand; isophthalaldehyde; DNA binding; Thiosemicarbazide.

1. Introduction

Thiosemicarbazide and its derivatives as ligands with potential sulphur and nitrogen donors are interesting and have gained special attention not only because of the structural chemistry of their multifunctional coordination modes, but also of their importance in medicinal and pharmaceutical field. They showed biological activities including antibacterial [1–3], antifungal [4,5], anticancer [6,7], antitumor [8, 9] and herbicidal activities [10]. The structure of the thiosemicarbazide moiety confers a good chelating capacity and this property can be increased in Thiosemicarbazone by inserting suitable aldehyde or ketone possessing a further donor atom to render the ligand polydentate [11]. Owing to the presence of the --NH-C=S functional group, Thiosemicarbazide exhibit thione-thiol tautomerism and can bind to the metal ion either in the anionic thiolate form or in the neutral thione form. Generally Thiosemicarbazide coordinate as bidentate ligand via azomethine nitrogen and thione/thiolate sulphur but when additional coordination functionality is present in the proximity of donating centres, the ligands will coordinate in a tridentate manner. During the last two or three decades, there has been an interesting attention on the binding study of small molecules to DNA, since it is an important genetic substance in organisms [12, 13]. Errors in gene expression can often cause disease and play a secondary role in the outcome and severity of human diseases [14]. A complete understanding of DNA – drug binding is significant in the rational design of DNA structural probe, DNA foot printing, sequence – specific cleaving agents and potential anti-cancer drugs [15]. Hence, it is essential to explore the interactions of metal complexes with DNA to design effective chemotherapeutic agents and better anticancer drugs. In the case of pharmaceuticals, the binding capacity of Thiosemicarbazones is further increased by condensation of the thiosemicarbazide with an aldehyde containing heteroatom [16, 17]. This aroused our interest in the synthesis of Cu(II), Co (II), Ni (II) and Zn (II) Thiosemicarbazide complexes. Herein, we report the synthesis, characterization, DNA binding and DNA cleavage, studies of the Schiff base obtained from 4-Aminoantipyrine with 1, 3-Isophthalaldehyde and Thiosemicarbazide and its metal (II) complexes. The investigation of the biological properties of the ligands and metal (II) complexes had been focused on the binding properties with CT-DNA performed by UV spectroscopy and cleavage properties of the complexes performed by gel electrophoresis with pBR322. Finally, we have studied their antifungal and antibacterial activity of the Schiff base ligand and their corresponding metal chelates is substitution dependent, mainly upon the chemical nature of the segment attached to the (C=S) carbon atom [18–21].

2. Experimental section

2.1. Materials and methods

All chemicals used in the present work viz., 4-Aminoantipyrine, 1,3-isophthalaldehyde, Thiosemicarbazide and metal(II) chlorides were chemically pure and AR grade. Commercial solvent (ethanol) was distilled and then used for the synthesis of ligand and its complexes. DNA was purchased from Bangalore Genei, Bangalore, India. The microanalyses (C, H, N) were performed in Carlo Erba 1108 analyzer at Sophisticated Analytical Instrument Facility (SAIF), Central Drug Research Institute (CDRI), Lucknow, India. Molar conductivities in DMSO (10^{-3} M) at room temperature were measured by using Systronic model-304 digital conductivity meter. The metal contents in the complexes were determined by standard EDTA titration [22]. Magnetic susceptibility measurement of the complexes was carried out by Gouy balance using copper sulphate pentahydrate as the calibrant. Infrared spectra ($4000\text{--}400\text{ cm}^{-1}$ KBr disc) of the samples were recorded on an IR Affinity-1 FT-IR Shimadzu spectrophotometer. NMR spectra were recorded in DMSO on a Bruker Avance Dry 300 FT-NMR spectrometer, using TMS as the internal reference. EPR spectra were recorded on a Varian E 112 EPR spectrometer in DMSO solution both at room temperature (300 K) and liquid nitrogen temperature (77 K). The absorption spectra were recorded by using Shimadzu model UV-1800 spectrophotometer at room temperature. Cyclic Voltammetric (CV) experiments were achieved on a CHI 620C

electrochemical analyzer in freshly distilled DMSO solution. Mass spectrometry experiments were performed on a JEOL-AccuTOF JMS-T100LC mass spectrometer equipped with a custom-made electro spray interface (ESI).

2.2. Synthesis

The synthesis of Schiff base ligand and its metal (II) complexes can be prepared by the method as follows.

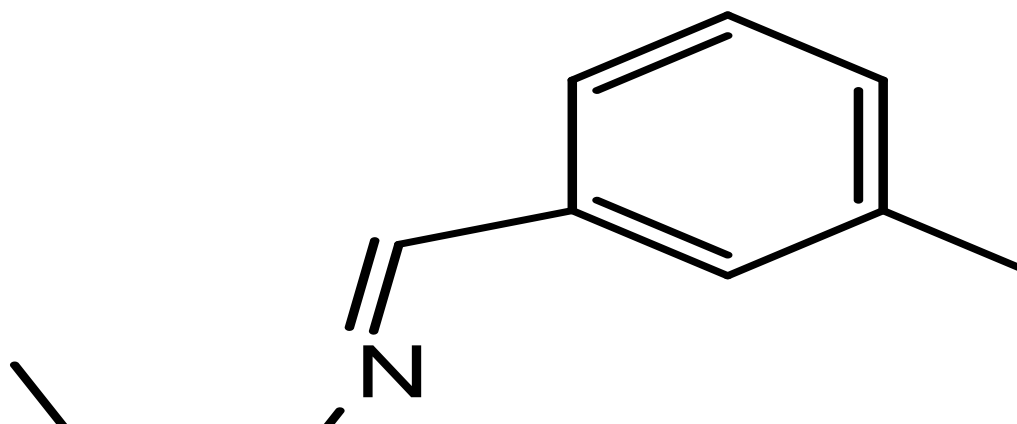
2.2.1. Synthesis of 1, 3-phenylene- bis-4-aminoantipyrine

The (1,3-phenylene- bis-4-aminoantipyrine) was prepared using the following method by condensation of 4-amino antipyrine (4.06 g, 10 mmol) dissolved in ethanol 30 mL was added to ethanolic solution of isophthalaldehyde (1.34 g, 5 mmol) (2: 1) mole ratio, and few drops of glacial acetic acid were added to reaction mixture with continuous stirring and refluxing at 60°C for (2 hr), the product precipitate was obtained by filtration and recrystallized from hot ethanol, and dried over anhydrous CaCl₂ (Scheme 1).

Scheme1. Synthesis of 1,3-phenylene- bis-4-aminoantipyrine

2.2.2. Synthesis of Schiff base (L)

The new Schiff base ligand (L) was prepared by condensation of 1,3-phenylene- bis-4-aminoantipyrine (5.05g, 10 mmol) was dissolved in 50 mL ethanol and refluxed with (1.82 g, 20 mmol) of thiosemicarbazide for (15 hr) adding three drops from glacial acetic acid. A clear yellow coloured solution was obtained. The Schiff base ligand was isolated after the volume of mixture was reduction to half by evaporation and recrystallized by hot ethanol and dried over anhydrous CaCl₂ (Scheme 2).



Ligand(L): Yield: 64%; pale yellow colour; Melting Point (108-110C°) ;Anal.Calc.for C₃₂H₃₄N₁₂S₂ (%): C(59.05), H (5.27); N (25.83) and S(9.85). Found (%): C (58.9), H (5.13); and N (25.03) ; FT-IR (KBr) (cm⁻¹): 1595 ν(C=N); 1145 ν(NH-C=S); 816 ν(C=S); 3368 ν(-NH₂) and 3251 ν(-NH-); ¹H NMR (DMSO) δppm: 6.9-8.5(m,Ar-H.), 2.21(s,

$\equiv\text{C}-\text{CH}_3$), 3.17 ($=\text{N}-\text{CH}_3$), 6.02(s,-NH₂), 10.8 (s,-NH-), and 9.78 (s,HC=N); MS m/z (%): 650 [M]⁺.UV-Vis. in DMSO, cm⁻¹ (transition): 37735 ($\pi-\pi^*$) and 31847 (n- π^*).

2.2.3. Synthesis of Schiff base metal(II) complexes (1-4)

The metal complexes were prepared by the mixing of (30 mL) ethanolic solution of the metal salt (1 mmol) namely (CoCl₂.6H₂O, NiCl₂. 6H₂O, CuCl₂.2H₂O, CuCl₂.2H₂O and ZnCl₂) with (0.65g, 1 mmol) of the ligand dissolved in (30 mL) ethanolic solution (1: 1) (metal: ligand) ratio. The resulting mixture was refluxed for (3 hr) with constant stirring. A coloured product appeared on standing and cooling the above solution. The precipitated solid complexes were filtered, washed with (5 mL) of hot ethanol to remove any traces of the unreacted starting materials. Finally, the complexes were dried under vacuum. Schematic route for the synthesis of Schiff base ligands (L) and its metal complexes (1-4) are present in **Figure 1**.



Figure 1. Proposed structure of the metal complexes M = Cu(II), Ni(II), Co(II) and Zn(II)

[CuL] (1): Yield: 58 %; black colour;Melting Point (122-124C°);Anal.Calc.for C₃₂H₃₄N₁₂S₂Cl₂Cu (%): C (48.94), H (4.36), N (21.40) and Cu (8.09); Found (%): C (48.04), H (4.26), N (21.22) and Cu (8.03); FT-IR (KBr) (cm⁻¹): 1583 $\nu(\text{C}=\text{N})$; 1124 $\nu(\text{NH}-\text{C}=\text{S})$; 772 $\nu(\text{C}=\text{S})$; 3364 $\nu(-\text{NH}_2)$; 3243 $\nu(-\text{NH}-)$; 544 (M-S) and 491 (M-N); \wedge_m ($\Omega^{-1}\text{mol}^{-1}\text{cm}^2$)135.7; μ_{eff} (BM) 1.75; MS m/z (%): 785 [M]⁺.UV-vis. in DMSO, cm⁻¹ (transition): 17,985 cm⁻¹ (d-d).

[CoL] (2): Yield: 54%; pink colour; Melting Point (128-130C°) ;Anal.Calc.for C₃₂H₃₄N₁₂S₂Cl₂Co (%): C (49.23), H (4.39), N (21.53) and Co (7.55); Found (%): C (49.1), H (4.17), N (20.58) and Co (7.48); FT-IR (KBr) (cm⁻¹): 1587 $\nu(\text{C}=\text{N})$; 1136 $\nu(\text{NH}-\text{C}=\text{S})$; 786 $\nu(\text{C}=\text{S})$; 3372 $\nu(-\text{NH}_2)$; 3245 $\nu(-\text{NH}-)$; 526 (M-S) and 486 (M-N); \wedge_m ($\Omega^{-1}\text{mol}^{-1}\text{cm}^2$)114.8; μ_{eff} (BM) 5.14; MS m/z (%): 780[M]⁺.UV-vis. in DMSO, cm⁻¹ (transition): 22,222 and 15290 (d-d).

[NiL](3):Yield:55%;Blackbrown colour;Melting Point (168-170C°);Anal.Calc.forC₃₂H₃₄N₁₂S₂Cl₂Ni (%): C (49.25), H (4.39), N (21.54) and Ni (7.52); Found (%): C (49.02), H (4.21), N (21.33) and Ni (7.45); FT-IR (KBr) (cm⁻¹) : 1588

$\nu(\text{C}=\text{N})$; 1132 $\nu(\text{NH}-\text{C}=\text{S})$; 794 $\nu(\text{C}=\text{S})$; 3366 $\nu(-\text{NH}_2)$; 3248 $\nu(-\text{NH}-)$; 539 (M-S) and 482 (M-N); Λ_m ($\Omega^{-1}\text{mol}^{-1}\text{cm}^2$) 94.2; μ_{eff} (BM) 2.87; UV-vis. in DMSO, cm^{-1} (transition): 21,505 and 14,104 (d-d).

[ZnL] (4): Yield: 60%; yellow colour; Melting Point ($132-134^\circ\text{C}$); Anal. Calc. for $\text{C}_{32}\text{H}_{34}\text{N}_{12}\text{S}_2\text{Cl}_2\text{Zn}$ (%): C (48.43), H (4.35), N (21.35) and Zn (8.31); Found (%): C (48.25), H (4.24), N (21.23) and Zn (8.23); FT-IR (KBr) (cm^{-1}): 1572 $\nu(\text{C}=\text{N})$; 1134 $\nu(\text{NH}-\text{C}=\text{S})$; 790 $\nu(\text{C}=\text{S})$; 3370 $\nu(-\text{NH}_2)$; 3246 $\nu(-\text{NH}-)$; 532 (M-S) and 480 (M-N); ^1H NMR (DMSO) δ ppm: 6.9-8.5(m, Ar-H), 2.21(s, $\equiv\text{C}-\text{CH}_3$), 3.17 (=N- CH_3), 6.02(s, - NH_2), 10.8 (s, -NH-), and 9.28 (s, HC=N); Λ_m ($\Omega^{-1}\text{mol}^{-1}\text{cm}^2$) 103.6; μ_{eff} (BM) diamagnetic; UV-vis. in DMSO, cm^{-1} (transition): 30,674 (LMCT).

2.3 DNA Binding Interaction

2.3.1. Absorption spectroscopic studies

The interaction between metal complexes and DNA was studied using electronic absorption, viscosity and electrochemical methods. Disodium salt of calf thymus (CT) DNA was stored at 4°C . All the experiments involving the interaction of the complexes with CT DNA were carried out in Tris-HCl buffer (50 mM Tris-HCl, pH 7.2) containing 5 % DMSO at room temperature. A solution of CT DNA in the buffer gave a ratio of UV absorbance at 260 and 280 nm of about 1.89, indicating the CT DNA sufficiently free from protein [23, 24]. The concentration of DNA was measured using its extinction coefficient at 260 nm ($6600 \text{ M}^{-1}\text{cm}^{-1}$) after 1:100 dilutions. Stock solutions were stored at 4°C and used not more than 4 days. Doubly distilled water was used to prepare solutions. Concentrated stock solutions of the complexes were prepared by dissolving the complexes in DMSO and diluting properly with the corresponding buffer to the required concentration for all the experiments. Absorption titration experiments were performed by maintaining a constant concentration of the complexes (30 μL), but varying the CT DNA concentration (0–180 μL) in buffer. After each addition of CT DNA to the complexes, the absorption readings were noted. The data were then fitted to the following equation (1) to obtain the intrinsic binding constant K_b values for interaction of the complexes with DNA [25,26].

$$[\text{DNA}] / (\epsilon_a - \epsilon_f) = [\text{DNA}] / (\epsilon_b - \epsilon_f) + 1 / [K_b((\epsilon_b - \epsilon_f))] \text{ ----- (1)}$$

In the above equation, [DNA] denotes the concentration of DNA, absorption coefficients ϵ_a , ϵ_f and ϵ_b correspond to $A_{\text{obs}}/[\text{complex}]$, free complex's extinction coefficient and the extinction coefficient of the complex in the totally bound form, respectively. From the equation (Eq. (1)), slope ($1/(\epsilon_b - \epsilon_f)$) and intercept ($1/[K_b(\epsilon_b - \epsilon_f)]$) were found out [27]. Finally by comparing the identified slope and intercept, K_b was calculated.

2.3.2. Cyclic Voltammetric Studies

Cyclic voltammetry studies were performed on a CHI 620C electrochemical analyzer with three electrode system of glassy carbon as the working electrode, a platinum wire as auxiliary electrode, Ag/AgCl as the reference electrode and 50 mM NaCl, 5 mM Tris buffer (pH 7.2). Solutions were deoxygenated by purging with N_2 for 30 min prior to measurements. [28]

2.3.3 Gel Electrophoresis Experiment

Interaction between the ligand and the complexes with pBR 322 plasmid DNA was studied by agarose gel electrophoresis. DNA cleavage activity of these compounds were monitored by using the reaction mixture containing 1 μg of plasmid DNA, 250 μg of sample, 2 μL of DMSO (1%) and 5 μL of hydrogen peroxide (40 mmol). The reaction mixture was incubated at 37°C for 3 h. After incubation, 2 μL of loading buffer (0.25% bromophenol blue, 0.25% xylene cyanol and 30% glycerol) was poured to a platform fixed with a comb to form slots and the

electrophoresis was performed at 50 V for 1 h in TBE (Tris-Borate EDTA) buffer using 1% agarose gel stained with ethidium bromide (1 μ g) and the bands were photographed.

2.4 Antimicrobial Screening

The *in vitro* antimicrobial screening of L and the complexes has been carried out against certain human sensitive pathogenic Gram-positive bacteria like *Staphylococcus aureus* and *Bacillus subtilis* and the Gram-negative bacteria such as *Salmonella typhi* and *Escherichia coli*. The fungi *Aspergillus niger*, *Cochliobolus lunatus*, *Rhizoctonia bataicola* and *Candida albicans* were tested by using broth micro dilution method [29]. The nutrient agar and dextrose agar were served as the medium for the growth of bacteria and fungi, Streptomycin and Nystatin were chosen as standards for antibacterial and antifungal activity, respectively. The samples were incubated at 37°C for 24 h (bacteria) and 48 h (fungi), respectively. The results were recorded in terms of MIC (Minimum Inhibitory Concentration). MIC is the lowest concentration of an antimicrobial compound that arrests the growth of a microorganism.

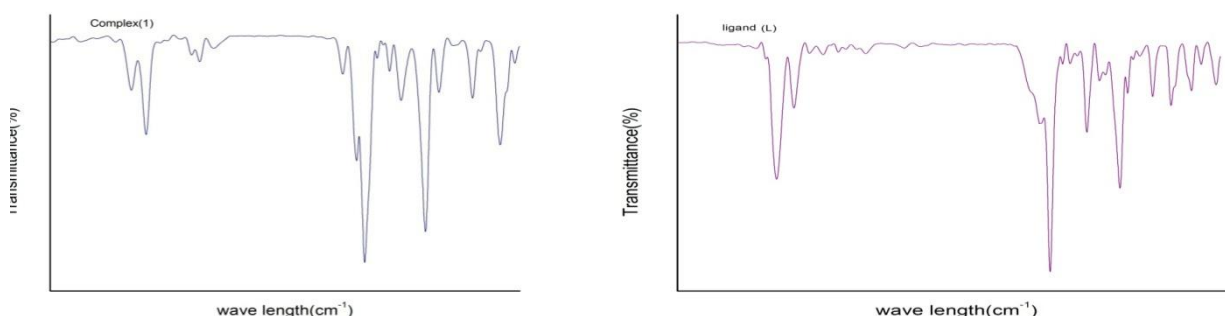
3. Results and discussion

The Schiff base ligand and its Cu(II), Ni(II), Co(II) and Zn(II) complexes have been synthesized and characterized by spectral and elemental analytical data. They are found to be air stable. The ligand is soluble in common organic solvents and all the complexes are freely soluble in CHCl_3 , DMF and DMSO but slightly soluble in methanol and ethanol and insoluble in water.

3.1. Elemental analysis and molar conductivity measurements

The elemental analysis results for the Schiff base and its metal complexes are in good agreement with the calculated values and also show that the complexes have 1:1 metal–ligand stoichiometry of the type $[\text{ML}]\text{Cl}_2$. The metal (II) complexes were dissolved in DMSO and the molar conductivities of 10^{-3} M of their solution at room temperature were measured. The higher conductance values ($135.7\text{--}94.2 \text{ S cm}^2 \text{ mol}^{-1}$) of the complexes support their electrolytic nature [30] implying the non-coordination of chloride anion to the central metal ion. The presence of counter chloride ion is confirmed from Volhard's test.

3.2. IR spectra



The IR absorption bands, which provide information about the formation of Schiff base ligand and the mode of coordination in its complexes, were given in the spectra (Figure.S1). In principle, the ligand can exhibit thione–thiol tautomerism since it contains a thioamide $-\text{NH}-\text{C}=\text{S}$ functional group. The $\nu(\text{S}-\text{H})$ band at 2565 cm^{-1} is absent in the IR spectrum of ligand but $\nu(\text{N}-\text{H})$ band at ca. 3214 cm^{-1} is present, indicating that in the solid state, the ligand remains as the thione tautomer. [31]The characteristic group of primary $\nu(-\text{NH}_2)$ and secondary amine $\nu(-\text{NH}-)$ of

thiosemicarbazide moiety, present in the Schiff base ligand was observed at 3368 cm^{-1} and 3251 cm^{-1} . The appearance of this band in all the metal (II) complexes indicates that the primary and secondary amine group is free from complexation. In the IR spectrum of the Schiff base ligand the band observed at 1595 cm^{-1} was shifted to lower frequency by $10\text{--}23\text{ cm}^{-1}$ on complexation, suggesting the coordination of the azomethine nitrogen. In addition, the ligand also revealed a band at 1656 cm^{-1} due to the $\nu(\text{C}=\text{N})$ vibration, originating from the condensation of amino group of thiosemicarbazide and 1,3-phenylene- bis-4-aminoantipyrine, was shifted by $11\text{--}23\text{ cm}^{-1}$ on complexation. [32,33]. This is also confirmed by the appearance of new bands in the range of $526\text{--}544\text{ cm}^{-1}$ and $480\text{--}491\text{ cm}^{-1}$ which may be due to $\nu(\text{M-N})$ and $\nu(\text{M-S})$ stretching vibrations, respectively [34]. The band appearing at 816 cm^{-1} corresponding to $\nu(\text{C}=\text{S})$ in the IR spectrum of ligand is shifted towards lower wave number by $22\text{--}44\text{ cm}^{-1}$ on complexation. It indicates that thione sulphur coordinates to the metal ion [35]. Thus, it may be concluded that the ligand behaves as a chelating agent coordinating through azomethine nitrogen and thiolate sulphur [36]. This discussion reveals that the Schiff base ligand possesses six potential coordination sites (SNNNNS) for Co(II), Ni(II) and Zn(II) complexes and four potential coordination sites (NNNN) for Cu(II) complex.

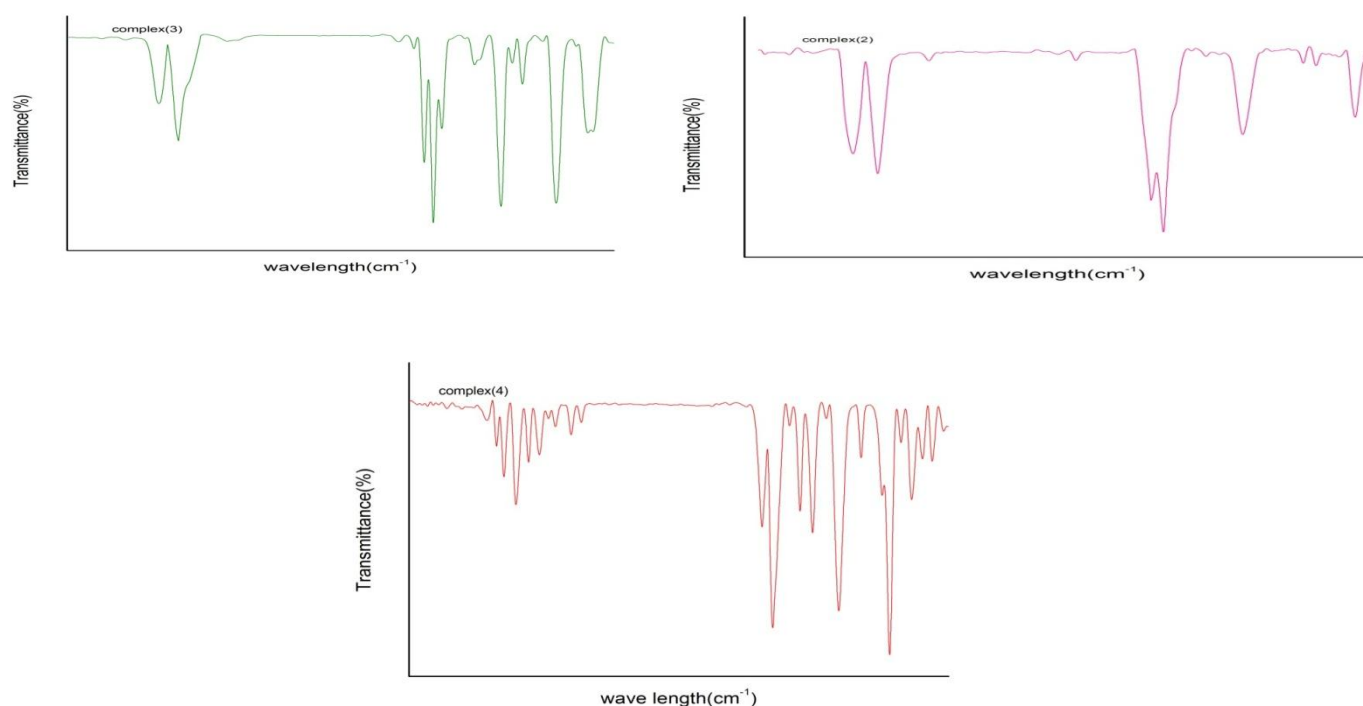


Figure S1. FT-IR spectra of ligand (L) and its M(II) [Cu, Co, Ni and Zn] complexes (1-4)

3.3 Magnetic moments and electronic spectra

The electronic spectra of the complexes were recorded in DMSO solution (Figure S2). The electronic spectra of the ligand show two intense bands at 37736 cm^{-1} and 31847 cm^{-1} . The first one at 37736 cm^{-1} , is assignable to a ligand $\pi \rightarrow \pi^*$ transitions while the other at 37736 cm^{-1} is due to $n \rightarrow \pi^*$ transitions associated with the imine function of the Schiff base [41]. In all metal complexes, the absorption bands are observed in the regions $37,037\text{--}37,736$ and $29,761\text{--}31,847\text{ cm}^{-1}$ which are due to $\pi \rightarrow \pi^*$ and $n \rightarrow \pi^*$ transitions. These transitions exhibit blue or red shift due to the coordination of the ligand with metal ions. The electronic spectra of $[\text{Cu}(\text{L})_2]$ complex exhibit the $d\text{--}d$ transition band in the region $17,986\text{ cm}^{-1}$ which is due to ${}^2\text{B}_{1g} \rightarrow {}^2\text{A}_{1g}$ transition. This $d\text{--}d$ band transition band strongly favours a square planar geometry around the metal ion. It is further supported by the magnetic moments value of (1.75 BM) [42, 43]. The nickel complex exhibits two $d\text{--}d$ bands at 21505 and 14104 cm^{-1} which are assigned as ${}^3\text{A}_{2g}(\text{F}) \rightarrow {}^3\text{T}_{1g}(\text{P})$ and

$^3A_{2g} \rightarrow ^3T_{1g}(F)$ transitions respectively, being characteristic of an octahedral geometry [44] supported by its magnetic susceptibility value (2.87 BM). The electronic spectrum of Co(II) complex showed two absorption bands at 22222 and 15290 cm^{-1} region, which are assignable to $^4T_{1g}(F) \rightarrow ^4T_{2g}(P)$ and $^4T_{1g}(F) \rightarrow ^4T_{2g}(F)$ transitions in an octahedral environment [45,46] which is also supported by its magnetic susceptibility value (5.14 BM). The complex of Zn(II) is diamagnetic. According to the empirical formula, an octahedral geometry is proposed for this complex.

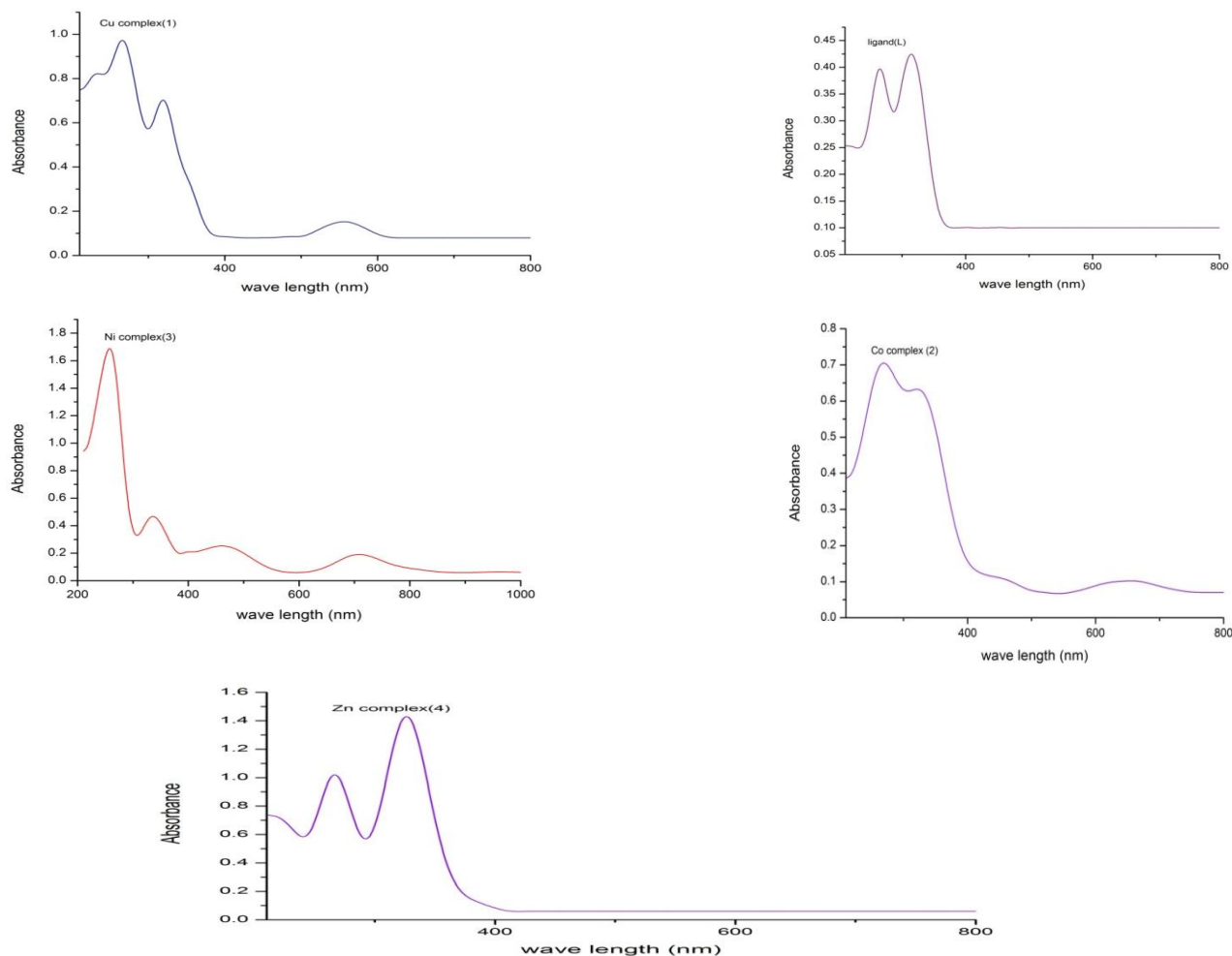


Figure S2. UV-Vis. spectra of Ligand (L) and its M(II) [Cu, Co, Ni and Zn] complexes (1-4)

3.4. ^1H NMR spectrum

The ^1H NMR spectra of Schiff base and its Zinc complex were recorded at room temperature in DMSO-d_6 solution used as a solvent. The ^1H NMR spectra of the Schiff base and its diamagnetic Zn (II) complex are shown in **Figure S3 and S4**. The ^1H NMR spectrum of the ligand shows a signal for the C-methyl proton ($\equiv\text{C-CH}_3$) attached to pyrazolone ring appear as a singlet at 2.44 ppm, while the N-methyl protons ($>\text{N-CH}_3$) attached to pyrazolone ring appear as a singlet at δ 3.17 ppm. In the ligand and the complex there is no significant change was observed [37]. In the ligand a sharp singlet at δ 6.02 ppm is due to $-\text{NH}_2$ group. The position of this singlet remains unchanged in the complexes. It shows that the $-\text{NH}_2$ group is not taking part in complexation [38]. The aromatic protons appear as a set of doublets, triplets and multiplets in the range of 6.9–8.5 ppm. Significant azomethine proton signal due to HC=N was observed at δ 9.78 ppm in Schiff base ligand. On complexation the position of this signal is shifted to δ 9.29 ppm. It indicates that

azomethine nitrogen involved in coordination. The proton peak of N–H group at δ 10.8 ppm remains at same position in ligand and in the complexes which suggests that deprotonation do not occurred [39].

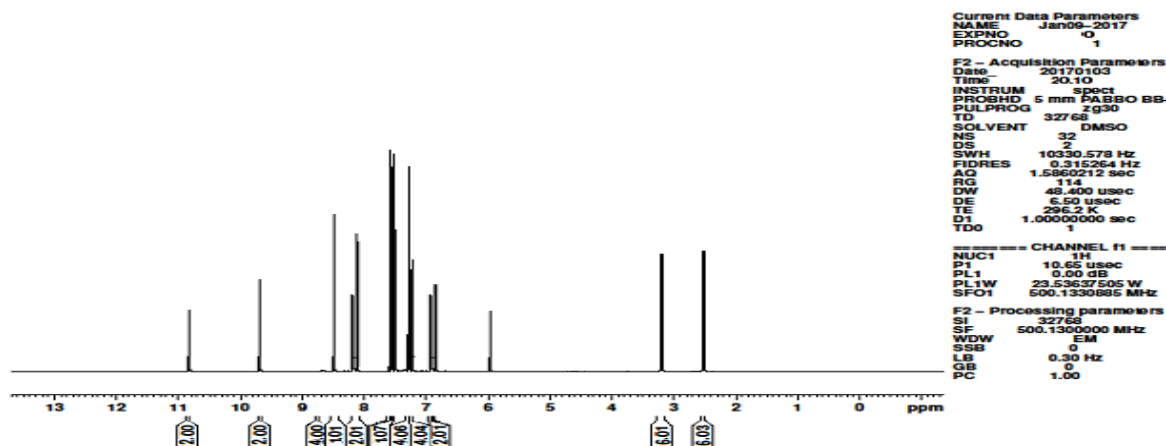


Figure S3. ^1H NMR spectrum of Ligand (L).

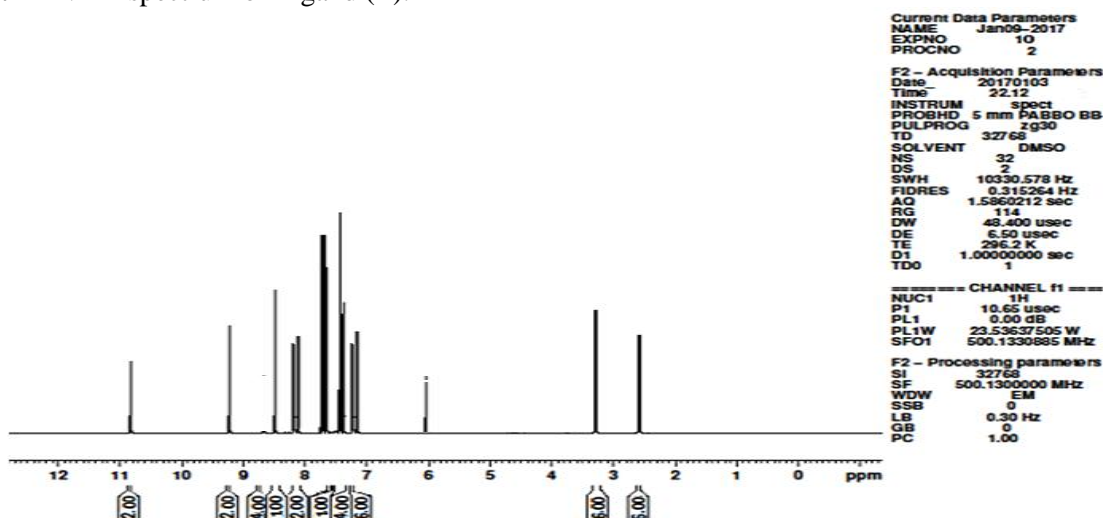


Figure S4. ^1H NMR spectrum of Zn(II) complex

3.5 Mass spectra

Mass spectra provide a vital role for elucidating the structure of compounds. The ESI mass spectrum of ligand L and its Cu and Co complexes were shown in Figure S5. The obtained molecular ion peaks confirmed the suggested formulae for the synthesized compounds. The mass spectrum of Schiff base ligand (L) shows the molecular ion peak at m/z 650 corresponding to $[\text{C}_{32}\text{H}_{34}\text{N}_{12}\text{S}_2]^+$ ion. Also the spectrum exhibits peaks for the fragments at m/z 274, 200, 123, 97, 77 and 75 corresponding to $[\text{C}_{12}\text{H}_{14}\text{N}_6\text{S}]^+$, $[\text{C}_{11}\text{H}_{12}\text{N}_4]^+$, $[\text{C}_5\text{H}_7\text{N}_4]^+$, $[\text{C}_5\text{H}_9\text{N}_2]^+$, $[\text{C}_6\text{H}_5]^+$ and $[\text{CH}_3\text{N}_2\text{S}]^+$ respectively. The spectrum of $[\text{Cu}(\text{L})]\text{Cl}_2$ complex shows molecular ion peak at m/z 785 $[\text{M} + 1]$ which is equivalent to its molecular weight similarly the spectrum of $[\text{Co}(\text{L})]\text{Cl}_2$ complex shows molecular ion peak at m/z 780, which is equivalent to its molecular weight. Both the $[\text{Cu}(\text{L})]\text{Cl}_2$ and $[\text{Co}(\text{L})]\text{Cl}_2$ complexes gives fragment ion peaks at m/z 274, 200, 123, 97, 77 and 75 corresponding to $[\text{C}_{12}\text{H}_{14}\text{N}_6\text{S}]^+$, $[\text{C}_{11}\text{H}_{12}\text{N}_4]^+$, $[\text{C}_5\text{H}_7\text{N}_4]^+$, $[\text{C}_5\text{H}_9\text{N}_2]^+$, $[\text{C}_6\text{H}_5]^+$ and $[\text{CH}_3\text{N}_2\text{S}]^+$ respectively. The m/z values of all the fragments of the ligands and their complexes confirm the stoichiometry of the complexes as $[\text{ML}]\text{Cl}_2$. The intensity of these peaks reflects the stability and abundance of the ions [40].

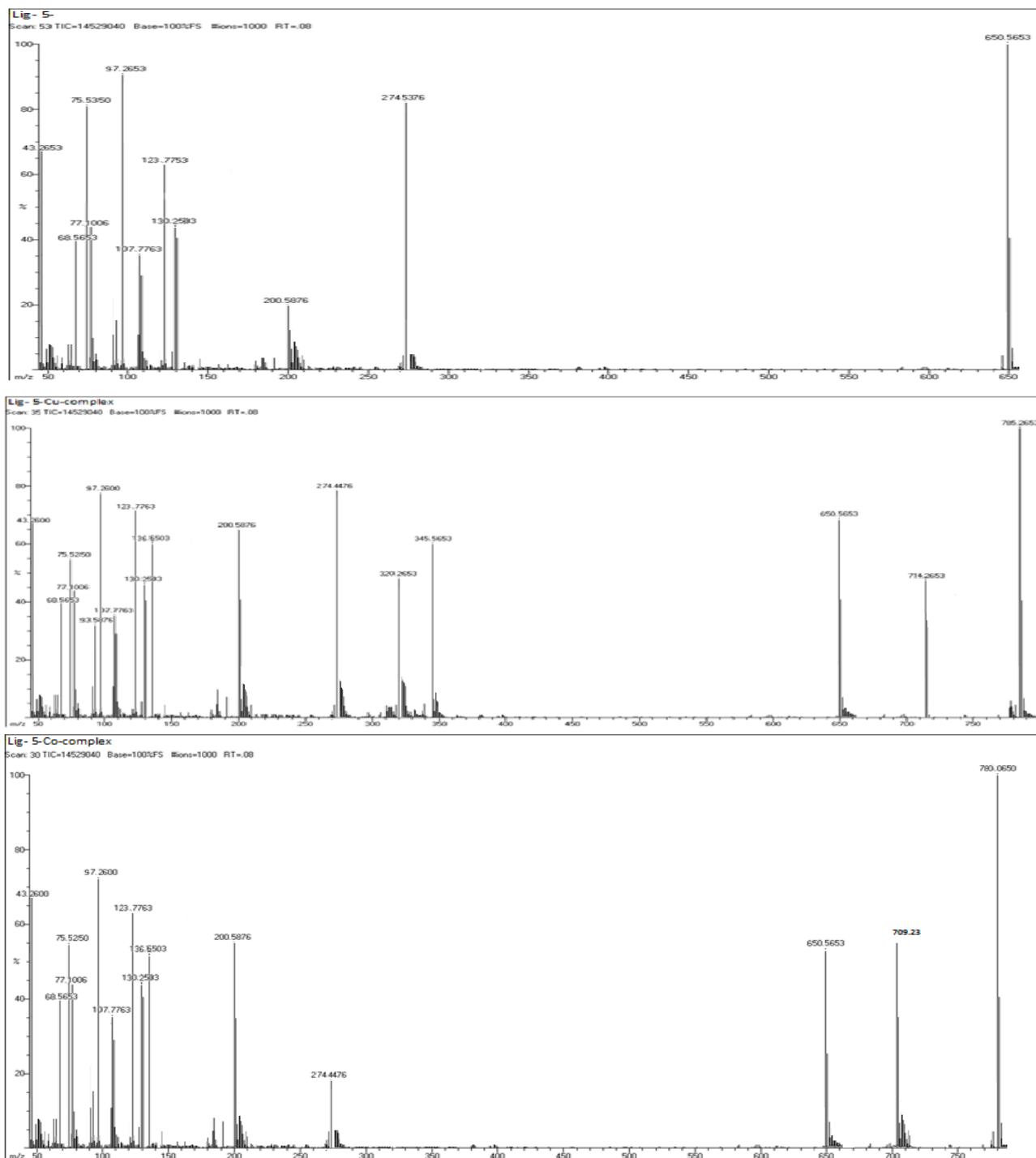


Figure S5. Mass spectrum of Ligand(L) and its Cu(II) and Co(II) complexes (1&2) .

3.6 EPR spectroscopy

ESR studies of paramagnetic transition metal (II) complexes yield information about the distribution of the unpaired electrons and hence about the nature of the bonding between the metal ion and its ligands. There have been many reports concerning the application of ESR to square planar or distorted octahedral complexes of Cu^{+2} and their interpretation of the ESR parameter in terms of covalence of M-L bonding. ESR spectra of copper complex recorded in DMSO solution at 300 and 77 K are shown in [figure S6](#). The spectrum of the Cu complex at 300 K shows one intense absorption band in the high field region and is isotropic due to the tumbling motion of the molecules [47]. The

spectrum consists of a set of four well resolved peaks in the low field region at 77K. The spin Hamiltonian parameters of the complexes were calculated (Table 1). The g_{\parallel} and g_{\perp} values are computed from the spectrum. The observed g_{\parallel} (2.2312) is less than 2.3 suggesting significant covalent character of the M-L bond [48]. The band g_{\parallel} (2.28) $>$ g_{\perp} (2.06) $>$ g_e (2.0023) suggests that the unpaired electron is localized in $d_{x^2-y^2}$ orbital for the copper complex and the four well resolved peaks of low intensities in the low field region in the frozen state at 77K, ruled out the Cu–Cu interaction. The g tensor values of Cu (II) complex can be used to derive the ground state. In tetragonal and square planar complexes, the unpaired electron lies in the $d_{x^2-y^2}$ orbital giving $^2B_{1g}$ as the ground state with the $g_{\parallel} > g_{\perp}$. From the observed values, it is clear that $g_{\parallel} > g_{\perp}$ (2.28 $>$ 2.06), which suggests that the complex is square planar [49, 50]. Also it is supported by the fact that the unpaired electron lies predominantly in the $d_{x^2-y^2}$ orbital for the copper complex, $g_{\parallel} = 2.28$, which is between 2.3–2.4 and thus in conformity with the presence of copper–nitrogen bonds in these chelates. Based on the above spectral and analytical data, the proposed structure of the Cu(II) complex is given in the (Figure 1).

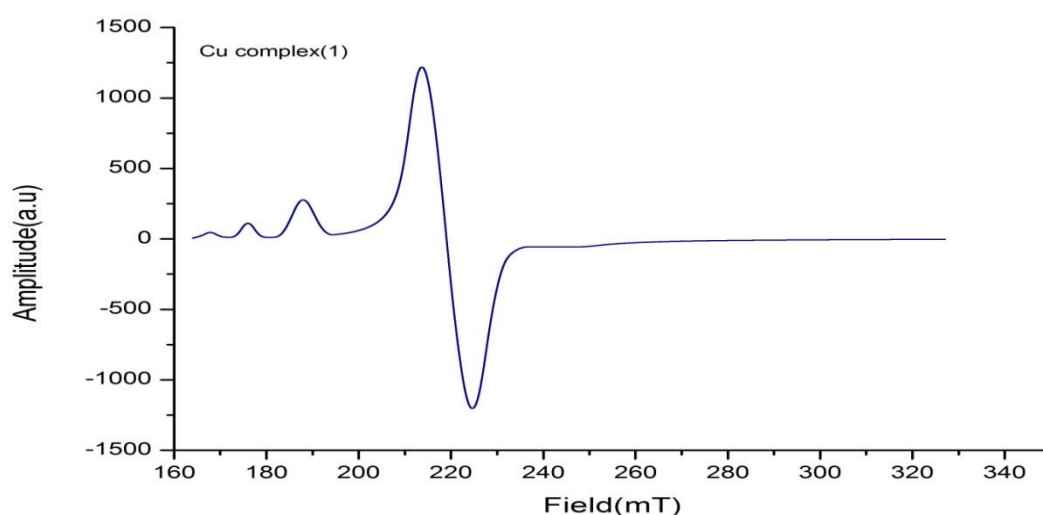


Figure S6. EPR spectrum of Cu(II) complex (1) at LNT

Table 1. The spin Hamiltonian parameters of the Cu(II) complex (1) in DMSO solution at LNT.

Complex	g-tensor		$A \times 10^{-4} \text{ (cm}^{-1}\text{)}$			G	
	g_{\parallel}	g_{\perp}	g_{iso}	A_{\parallel}	A_{\perp}		A_{iso}
copper	2.28	2.06	2.13	123	19	54	4.6

3.7. DNA binding experiments

3.7.1. Absorption titration

The electronic absorption spectroscopy is the most common way to investigate the interactions of complexes with DNA. In general, complex bound to DNA (CT-DNA) through intercalation usually results in hypochromism and red shift (bathochromism), due to the strong stacking interaction between aromatic chromophore of the complex and the base pairs of DNA. The Ni(II) and Zn(II) complexes showed absorption bands at 344 nm and 337nm, With increasing concentration of DNA, all the complexes showed hypochromicity and a red-shifted charge transfer peak maxima in the absorption spectra. The absorption spectra of Ni(II) and Zn(II) complexes in the absence and presence of CT-DNA

are given in Figure 2. These spectroscopic characteristics suggest that the complexes interact with DNA most likely through a mode that involves a stacking interaction between the aromatic chromophore and the base pairs of DNA [51]. If the binding mode is intercalation, the π^* orbital of the intercalated ligand can couple with the π orbital of the DNA base pairs, thus, decreasing the π - π^* transition energy and resulting in the bathochromism. To compare quantitatively the affinity of the two complexes toward DNA, the intrinsic binding constants K_b of the two complexes to CT-DNA were determined by monitoring the changes of absorbance, with increasing concentration of DNA. The calculated K_b values are given in Table 2. The determined intrinsic binding constants for [CuL], [CoL], [NiL] and [ZnL] are $8.5 \times 10^5 \text{ M}^{-1}$, $5.2 \times 10^5 \text{ M}^{-1}$, $6.6 \times 10^5 \text{ M}^{-1}$ and $7.6 \times 10^5 \text{ M}^{-1}$, respectively. Hence, it shows that the observed K_b value of the present complexes is higher than that of cisplatin ($5.73 \times 10^4 \text{ M}^{-1}$) [52] and relatively lower than the metallointercalator $[\text{Ru}(\text{bpy})_2(\text{HBT})]^{2+}$ ($5.71 \times 10^7 \text{ M}^{-1}$) [53].

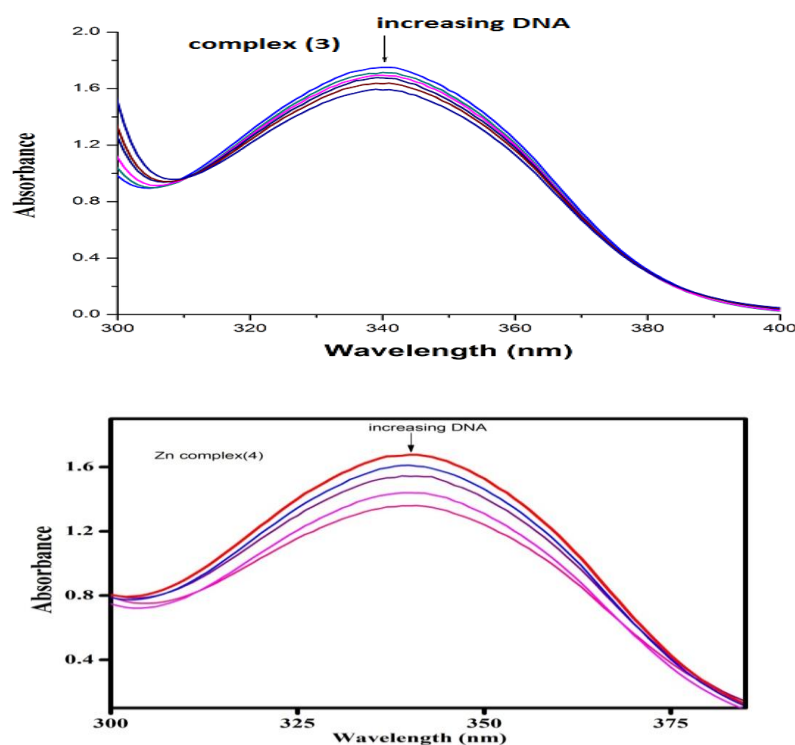


Figure 2. Absorption spectra of complexes (3) and (4) in buffer pH=7.2 at 25 °C in presence of increasing amount of DNA. Arrow indicates the changes in absorbance upon increasing the DNA concentration.

Table 2. Electronic absorption parameters for the interaction of DNA with synthesized complexes.

Complex	λ max		$\Delta\lambda$ (nm)	$^a\text{H}\%$	$K_b \times 10^5 (\text{M}^{-1})$
	Free	Bound			
Cu	267	269	2.0	15.6	8.5
Co	248	250	2.0	0.85	5.2
Ni	340	342	2.0	0.56	6.6
Zn	340	341	1.0	13.5	7.6

$$^a\text{H}\% = [(A_{\text{free}} - A_{\text{bound}}) / A_{\text{free}}] \times 100\%$$

3.7.2 Cyclic Voltammetry

To assist the nature of binding of the complexes with DNA, cyclic voltammetry technique has been carried out in the absence and presence of DNA with varying concentrations and the data are presented in Table 3. With the addition of CT-DNA to the complexes, the voltammetric current coupled with positive shift in $E_{1/2}$ is observed to decrease significantly. The cyclic voltammograms for complexes 3 and 4 in the presence and absence of varying concentrations of DNA are shown in (Figure 3). When the complex binds with DNA, a non-electro active product is formed which decreases the concentration of the electro active species present in the solution thereby causing a drop in the peak current [54]. In this case, the drop of Voltammetric current in the presence of DNA may be attributed to slow diffusion of the metal complex bound to CT DNA. The positive shift of E_{pc} or E_{pa} indicates that the complex intercalates into DNA double helix [55].

Table 3. Electrochemical parameters for the interaction of DNA with synthesized metal complexes.

Complex	$E_{1/2}(V)^a$		$^b \Delta E_p(V)$		I_{pa}/I_{pc}
	Free	Bound	Free	Bound	
Cu	-0.202	0.156	-0.785	0.562	0.85
Co	-0.562	0.265	0.256	1.236	0.88
Ni	-0.678	-0.602	1.365	2.035	0.68
Zn	-0.296	-0.778	3.691	0.962	0.72

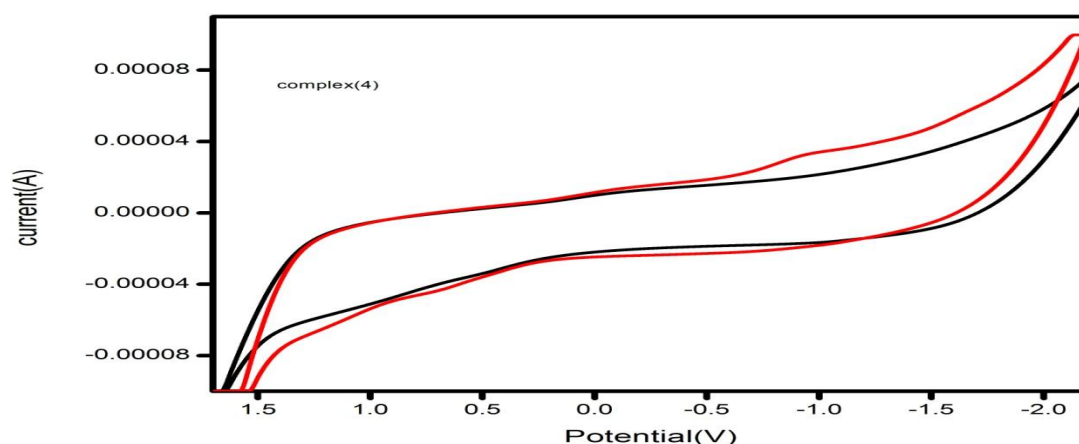


Figure 3. Cyclic voltammogram of complexes (3) and (4) in buffer (pH = 7.2) at 25°C in presence of increasing amount of DNA.

3.7.3 DNA cleavage efficacy

The efficacy of the metal complexes to act as artificial nucleases is monitored by subjecting the super coiled plasmid DNA pBR322 to agarose gel electrophoresis [56]. The super coiled DNA is said to relax into nicked form and linear form due to the double strand cleavage by the metal complexes. The Figure 4 displays the cleavage pattern of pBR322 DNA in the presence of metal complexes and H_2O_2 . It is duly noted that neither the ligand nor the control showed effective activity as the DNA remained uncleaved, whereas subsequent activity can be found in the lanes containing metal complexes. The complexes 1 and 4 showed superior activity by cleaving into distinctive nicked (open circular)

and linear form. The double strand cleavage of the plasmid DNA was prominent with the increase in the concentration of the metal complexes suggesting the nuclease activity of the metal complexes [57]. It can be deduced from the obtained results that the metal complexes may be considered as potential concentration dependent nuclease agents.

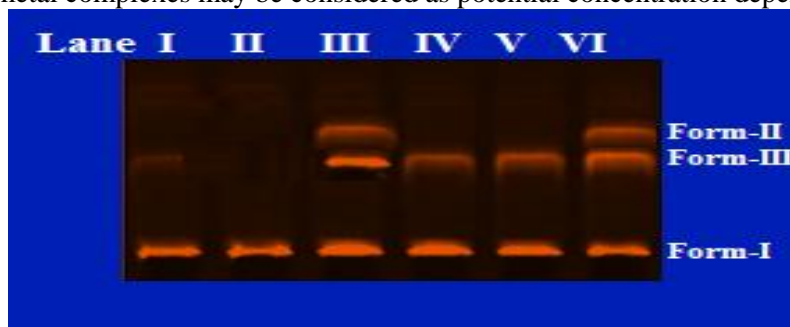


Figure 4. Gel electrophoresis pattern showing cleavage of pBR 322 DNA treated with metal complexes. Lane I; DNA control; Lane II: DNA + L+ H₂O₂; Lane III: DNA + [CuL]Cl₂ + H₂O₂; Lane IV: DNA + [CoL]Cl₂ + H₂O₂; Lane V: DNA + [NiL]Cl₂ + H₂O₂ and Lane VI: DNA + [ZnL]Cl₂ + H₂O₂.

3.8. Antimicrobial screening

3.8.1. Antibacterial activity

The reactivity of the synthesized compounds towards the biological systems is an important feature of the current research and Schiff bases of transition metal complexes (1-4). All the synthesized compounds (Table 4) showed a remarkable biological activity against all the bacterial species of *Staphylococcus aureus*, *Bacillus subtilis*, *Escherichia coli*, and *Salmonella typhi*, under investigation by paper disc method. The effectiveness of the investigated ligand and its metal complexes as good antimicrobial agents has been screened in addition to evaluation of few known antibiotics using streptomycin as standard antibacterial agent. The results indicate that the ligand exhibits moderate antibacterial activity with respect to the complexes against the same microorganisms under identical experimental conditions owing to the theory of Tweedy [58]. Further, the antibacterial action of Schiff base ligand may be significantly enhanced on the presence of azomethine groups(C=N-) and the sulphur moiety(C=S) of thiosemicarbazide both of which have chelating properties. These properties may be used in metal transport across the bacterial membranes or to attach to the bacterial cells at a specific site from which it can interfere with their growth. Ligand exhibits MIC in the range of (10.8–12.5 µg/mL) against all the pathogens. The metal(II) complexes shows better antibacterial activity (MIC, 1.7–3.5 µg/mL) against the tested microorganisms. Such increased activity of the metal chelates can be explained on the basis of Overtone's concept [59] and Tweedy's chelation theory [60]. According to Overtone's concept of cell permeability the lipid membrane that surrounds the cell favours the passage of lipid soluble materials due to which liposolubility is an important factor which controls the antimicrobial activity. On chelation, the polarity of the metal ion will be reduced to a greater extent due to the overlap of the ligand orbital and partial sharing of positive charge of the metal ion with donor groups. Further, it increases the delocalization of π -electrons over the whole chelate ring and enhances the lipophilicity of the complex. This increased lipophilicity enhances the penetration of the complexes into lipid membrane and blocks the metal binding sites on enzymes of microorganisms.

Table 4. The in vitro antibacterial activity of Schiff base and its metal complexes (MIC in µg/mL).

Compound	Minimum inhibitory concentration (MIC)			
	<i>A.niger</i> <i>C.albicans</i>	<i>C.lunata</i>	<i>R.bataticola</i>	
L	11.5	13.2	10.2	12.8
1	2.1	2.4	2.9	5.2
2	3.5	3.9	3.6	4.4
3	4.2	5.1	5.4	6.0
4	4.5	5.3	5.7	5.9
Nystatin	1.2	1.7	1.3	2.0

Streptomycin is used as the standard. MIC (µg/mL) minimum inhibitory concentration, i.e. the lowest concentration to completely inhibit the bacterial growth.

3.8.2. Antifungal activity

The Schiff base and its metal complexes were screened for their antifungal activity against *A. niger*, *C. lunata*, *R. Bataicola* and *C. albicans*. The minimum inhibitory concentration (MIC) values of the investigated compounds are summarized in (Table 5).

Table 5. The in vitro antifungal activity of Schiff base and its metal complexes (MIC in µg/mL)

Compound	Minimum inhibitory concentration (MIC)			
	<i>S.aureus</i>	<i>B.subtilis</i>	<i>E.coli</i>	<i>S.typhi</i>
L	10.8	11.6	12.5	11.1
1	1.7	2.1	2.3	1.9
2	2.3	2.7	2.6	2.4
3	2.5	2.9	3.2	3.3
4	2.8	3.4	3.0	3.5
Streptomycin	1.0	1.1	1.3	1.2

The effectiveness of the investigated ligand and its metal complexes as good antimicrobial agents has been screened in addition to evaluation of few known antibiotics using Nystatin as standard antifungal agent. A comparative study of MIC values of ligand (10.2–13.2µg/mL) and its complexes (2.1–6.0µg/mL) against all the fungi indicates that the metal complexes exhibit higher antifungal activity than the ligand. It was evident from the data that this activity significantly increased on coordination. This enhancement in the activity may be rationalized on the basis that their structures mainly possess an additional (=C=N-) and (C=S) bonds. It has been suggested that the ligands with nitrogen and sulphur donor systems inhibit enzyme activity, since the enzymes which require these groups for their activity appear to be especially more susceptible to deactivation by metal ions on coordination. Moreover, coordination reduces the polarity [61] of the metal ion mainly because of the partial sharing of its positive charge with the donor groups [62] within the chelate ring system formed during coordination. This process, in turn, increases the lipophilic nature of the central metal atom, which favours its permeation more efficiently through the lipid layer of the

microorganism [63], thus destroying them more aggressively. Nystatin is used as the standard. MIC ($\mu\text{g/mL}$) minimum inhibitory concentration, i.e., the lowest concentration to completely inhibit the fungal growth.

4. Conclusion

In this paper, the coordination chemistry of a Schiff base ligand (L) obtained from the condensation of 4-Aminoantipyrine with 1, 3-Isophthalaldehyde and Thiosemicarbazide. The Schiff base ligand and its metal complexes of Co(II), Ni(II), Cu(II) and Zn(II) were synthesized and characterized by spectral and analytical data. Elemental analysis and high molar conductance values indicate mononuclear and electrolytic nature of the complexes. The Schiff base acts as a both tetradentate and hexadentate ligand, and the possible coordination sites are six potential coordination sites (SNNNNS) for Co(II), Ni(II) and Zn(II) complexes and four potential coordination sites (NNNN) for Cu(II) complex. Spectral data and magnetic moment studies suggest that cobalt (II), nickel (II), and zinc (II) complexes have octahedral geometry, while the copper (II) complex has square planar geometry. The DNA-binding properties of synthetic metal complexes have been comprehensively studied by different methods including electronic absorption spectra and cyclic voltammetry. The experimental results reveal that all the complexes can interact with DNA through intercalation mode. The complexes are capable of cleaving pBR 322 DNA in the presence of H_2O_2 . The antimicrobial studies show that the complexes are more active than the ligand.

Acknowledgement

The authors express their sincere thanks to the Principal and the Management Committee HKRH College, Uthamapalayam for their constant encouragement. We extend our hearty thanks to the Management committee, The Madura College, Madurai for providing research facilities.

References

1. P.G. More, R.B. Bhalvankar, S.C. Pattar, *J. Indian Chem. Soc.* 78 (2001) 474.
2. A.H. El-Masry, H.H. Fahmy, S.H.A. Abdelwahed, *Molecules* 5 (2000) 1429.
3. M.A. Baseer, V.D. Jadhav, R.M. Phule, Y.V. Archana, Y.B. Vibhute, *Orient. J. Chem.* 16 (2000) 553.
4. S.N. Pandeya, D. Sriram, G. Nath, E.D. Clercq, *II Farmaco* 54 (1999) 624.
5. W.M. Singh, B.C. Dash, *Pesticides* 22 (1988) 33.
6. S.B. Desai, P.B. Desai, K.R. Desai *Heterocycl. Commun.* 7 (2001) 83.
7. P. Pathak, V.S. Jolly, K.P. Sharma, *Orient. J. Chem.* 16 (2000) 161.
8. M. Das and S.E. Livingstone, *Inorg. Chim. Acta* 19 (1976) 5.
9. M. Mohan, A. Aganval, N.K. Jha, *J. Inorg. Biochem.* 34 (1981) 41.
10. S. Samadhiya, A. Halve, *Orient. J. Chem.* 17 (2001) 119.
11. M. Belicchi-Ferrai, F. Biscegli, G. Pelosi, S. Pinelli, P. Tarascani, *Polyhedron* 26,(2007) 5150.
12. K.E. Erkkila, D.T. Odon, J.K. Barton, *Chem. Rev.* 99 (1999) 2777.
13. A. Chouai, S.E. Wicke, C. Turro, J. Bacsá, K.R. Dunbar, D. Wang, R.P. Thummel, *Inorg. Chem.* 44 (2005) 5996.
14. J. Hooda, D. Bednar ski, L. Irish, S.M. Firestine, *Med. Chem.* 14 (2006) 1902.
15. V. Uma, V.G. Vaidyanathan, B.U. Nair, *Bull. Chem. Soc. Jpn.* 78 (2005) 845.
16. R.N. Prabhu, D. Pandiarajan, R. Ramesh, *J. Organomet. Chem.* 694 (2009) 4170.
17. J.S. Casas, M.S. Garcia-Tasende, J. Sordo, A structural review, *Coord. Chem. Rev.* 209 (2000) 197.
18. D.X. West, C.S. Carlson, A.C. Whyte, E.E. Liberta, *Trans. Met. Chem.* 15 (1990) 43.
19. D.X. West, C.S. carlion, G.P. sollowa, C.R. Daniel, *Trans. Met. Chem.* 15 (1990) 91.

20. D.X. West, C.S. Carlson, A.E. Liberta, C.R. Daniel, *Trans. Met. Chem.* 5 (1990) 341.
21. D.X. West, C.S. Carlson, A.E. Liberta, J.P. Scovill, *Trans. Met. Chem.* 15 (1991) 383.
22. A.I. Vogel, A Textbook of Quantitative Inorganic Analysis Including Elementary Instrumental Analysis, 4th ed., Longman, London, (1978).
23. J. Marmur, *J. Mol. Biol.* 3 (1961) 208.
24. M.E. Reichmann, S.A. Rice, C.A. Thomas, P. Doty, *J. Am. Chem. Soc.* 76 (1954) 3047.
25. C.V. Kumar, E.H. Asuncion, *J. Am. Chem. Soc.* 115 (1993) 8547.
26. A. Wolfe, G.H. Shimer, T. Meehan, *Biochem.* 26 (1987) 6392.
27. J.B. Chaires, N. Dattagupta, D.M. Crothers, *Biochemistry*, 21 (1982) 3933.
28. M. Mariappan, M. Suenaga, A. Mukhopadhyay, B.G. Maiya, *Inorg. Chim. Acta* 390 (2012) 95.
29. M. Sonmez, M. Celebi, I. Berber, *Eur. J. Med. Chem.* 45 (2010) 1935.
30. WJ. Geary, *Coord. Chem. Rev.* 7 (1971) 81.
31. S. Chandra, S. Bargujar, R. Nirwal, N. Yadav, *Spectrochim. Acta A* 106 (2013) 91.
32. K.P. Deepa, K.K. Aravindakshan, *Syn. React. Inorg. Met. Org.* 30 (2000) 1601.
33. M. Joseph, A. Sreekanth, V. Suni, M.R.P. Kurup, *Spectrochim. Acta A* 64 (2006) 637.
34. S. Chandra, L.K. Gupta, *Spectrochim. Acta A* 61 (2005) 269.
35. N.S. Youssef, K.H. Hegab, *Synth. React. Inorg. Met. Org. Chem.* 35 (2005) 391–399.
36. U. Kumar, S. Chandra, *Synthesis*, *J. Saudi Chem. Soc.* 15 (2011) 187–193.
37. N. Raman, S. Sobha, *Spectrochim. Acta A* 78 (2011) 888.
38. S. Chandra, S. Bargujar, R. Nirwal, N. Yadav, *Spectrochim. Acta A* 106 (2013) 91.
39. F.W. Wehrli, A.P. Marchand, S. Wehrli, *Interpretation of Carbon-13NMR Spectra*. 2nd Edition, Wiley, New York (1988).
40. M. Hamming, N. Foster, Academic Press: New York, USA, (1972).
41. D.X. West, A.A. Nasar, *Trans. Met. Chem.* 24 (1999) 617.
42. L.N. Sharadha, M.C. Ganorkar, *Indian J. Chem.* 27 (1988) 617.
43. M.S. Nair, S.T. David, M. Anbu, *Indian J. Chem.* 38A (2001) 823.
44. A.I. Vogel, A Textbook of Quantitative Inorganic Analysis, fourth ed., ELBS and Longman, (1978).
45. J.K. Nag, S. Pal, C. Sinha, *Trans. Met. Chem.* 30 (2005) 523.
46. M.M. Omar, G.G. Mohamed, *Spectrochim. Acta A* 61 (2005) 929.
47. R.K. Ray, G.B. Kauffman, *Inorg. Chim. Acta* 173 (1990) 207.
48. A.H. Maki, B.R. McGarvey, *J. Chem. Phys.* 29 (1958) 31.
49. M.A. Halcrow, L.M. Chia, X. Liu, E.J.L. McIner, J.E. Davies, *Chem. Commun.* 22 (1998) 2465.
50. P. Mishra, M. Khare, S.K. Gautam, *Synth. React. Inorg. Met. Org. Chem.* 32 (2002) 1485.
51. B. Peng, Z. Wen-Hui, L. L. Yan, Han-Wen, L. Zhu, *Trans. Met. Chem.* 34 (2009) 231.
52. C.N. N'soukpoe-Kossi, C. Descoteaux, E. Asselin, H.A.T. Riahi, G. Berube, *DNA and Cell Biol.* 27 (2008) 101.
53. D.L. Arockiasamy, S. Radhika, R. Parthasarathi, B.U. Nair, *Eur. J. Med. Chem.* 44 (2009) 2044.
54. J.M. Kelly, E.G. Lyons, J.M.V. Putten, R.E. Smyth, Amsterdam, Elsevier, 25 (1986) 205.
55. S.S. Zhang, S.Y. Niu, B. Qu, G.F. Jie, H. Xu, C.F. Ding, *J. Inorg. Biochem.* 99 (2005) 2340.
56. R. Paulpandiyam, N. Raman, *Appl. Organomet. Chem.* 30 (2016) 531.
57. S. Sathiyaraj, K. Sampath, R.J. Butcher, R. Pallepogu, C. Jayabalakrishnan, *Eur. J. Med. Chem.* 64 (2013) 81.
58. B.G. Tweedy, *Phytopathology* 55 (1964) 910.
59. S. Belaid, A. Landreau, S. Djebbar, O. Benali-Baitich, G. Bouet, J.P. Bouchara, *J. Inorg. Biochem.* 102 (2008) 63.

60. N. Dharamaraj, P. Viswanathamurthi, K. Natarajan, *Trans. Met. Chem.* 26 (2001) 105.
61. B.N. Meyer, N.R. Ferrigni, J.E. Putnam, L.B. Jacobsen, D.E. Nichols, J.L. McLaughlin, *Planta Med.* 45 (1982) 31.
62. Z.H. Chohan, C.T. Supuran, A. Scozzafava, *J. Enzyme Inhib. Med.Chem.* 19 (2004) 79.
63. Z.H. Chohan, M. Praveen, , *Appl. Organomet. Chem.* 15 (2001) 617.